AD-A207 459 A STUDY OF THE ISOTHERMAL CRYSTALLIZATION KINETICS OF POLY(BIS(TRIFLUOROE..(U) PITTSBURGH UNIV PA SCHOOL OF ENGINEERING R J CIORA ET AL. 01 MAY 89 1/1

UNCLASSIFIED N00014-85-K-0358 F/G 7/6 NL

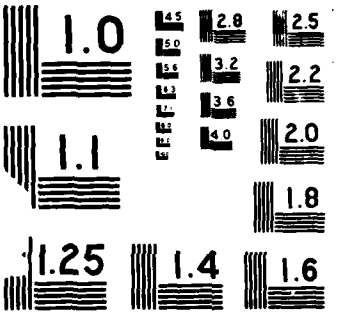
1.0
4.5
5.0
5.6
6.3
2.8
3.2
3.6
4.0
2.5
2.2
2.0
1.8
1.1
1.25
1.4
1.6

A STUDY OF THE ISOTHERMAL CRYSTALLIZATION KINETICS OF POLY[BIS(TRIFLUOROETHOXY)PHOSPHAZENE] AND POLY[BIS(PHENYLPHENOXY)PHOSPHAZENE]

R. J. Ciora Jr. and J. H. Magill

School of Engineering, University of Pittsburgh

Pittsburgh, PA 15261 USA

ABSTRACT

The kinetics of isothermal crystallization of two polyphosphazene polymers, poly[bis(trifluoroethoxy)phosphazene] and poly[bis(phenylphenoxy)phosphazene], have been studied utilizing a modified differential scanning calorimeter (DSC) technique and the depolarized light intensity (DLI) technique. The kinetics of transformation of both the isotropic to 2-D pseudo-hexagonal mesophase as well as the mesophase to 3-D orthorhombic phases have been measured and analyzed using Avrami theory. Classical nucleation theory has been utilized for estimating values of the surface free energies of the nuclei during crystallization.

Key Words:

Crystallization, Phase Transformation, Thermotropic Mesophase

SECURITY CLASSIFICATION OF THIS PAGE

REPORT DOCUMENTATION PAGE

1a. REPORT SECURITY CLASSIFICATION None	1b. RESTRICTIVE MARKINGS None
2a. SECURITY CLASSIFICATION AUTHORITY None	3. DISTRIBUTION / AVAILABILITY OF REPORT Unlimited
2b. DECLASSIFICATION / DOWNGRADING SCHEDULE None	
4. PERFORMING ORGANIZATION REPORT NUMBER(S) ONR Report #10	5. MONITORING ORGANIZATION REPORT NUMBER(S) ONR N00014-85-K-0358
6a. NAME OF PERFORMING ORGANIZATION University of Pittsburgh 6b. OFFICE SYMBOL (If applicable)	7a. NAME OF MONITORING ORGANIZATION Office of Naval Research
6c. ADDRESS (City, State, and ZIP Code) 848 Benedum Hall (School of Engineering) University of Pittsburgh Pittsburgh, PA 15261	7b. ADDRESS (City, State, and ZIP Code) 800 N. Quincy Avenue Arlington, VA 22217
8a. NAME OF FUNDING / SPONSORING ORGANIZATION Office of Naval Research 8b. OFFICE SYMBOL (If applicable)	9. PROCUREMENT INSTRUMENT IDENTIFICATION NUMBER
8c. ADDRESS (City, State, and ZIP Code) 800 N. Quincy Avenue Arlington, VA 22217	10. SOURCE OF FUNDING NUMBERS PROGRAM ELEMENT NO. / PROJECT NO. / TASK NO. / WORK UNIT ACCESSION NO.

11. TITLE (Include Security Classification) A Study of the Isothermal Crystallization Kinetics of Poly[bis-(trifluoroethoxy)phosphazene] and Poly[bis(phenylphenoxy)phosphazene]

12. PERSONAL AUTHOR(S) R. J. Ciora Jr. and J. H. Magill

13a. TYPE OF REPORT	13b. TIME COVERED	14. DATE OF REPORT (Year, Month, Day)	15. PAGE COUNT
Technical	FROM 1988 TO 89	5/1/89	

16. SUPPLEMENTARY NOTATION

17. COSATI CODES			18. SUBJECT TERMS (Continue on reverse if necessary and identify by block number)
FIELD	GROUP	SUB-GROUP	

19. ABSTRACT (Continue on reverse if necessary and identify by block number)

The kinetics of isothermal crystallization of two polyphosphazene polymers, poly[bis(trifluoroethoxy)phosphazene] and poly[bis(phenylphenoxy)phosphazene], have been studied utilizing a modified differential scanning calorimeter (DSC) technique and the depolarized light intensity (DLI) technique. The kinetics of transformation of both the isotropic to 2-D pseudo-hexagonal mesophase as well as the mesophase to 3-D orthorhombic phases have been measured and analyzed using Avrami theory. Classical nucleation theory has been utilized for estimating values of the surface free energies of the nuclei during crystallization.

Key Words:

Crystallization, Phase Transformation, Thermotropic Mesophase

20. DISTRIBUTION / AVAILABILITY OF ABSTRACT ☒ UNCLASSIFIED/UNLIMITED ☒ SAME AS RPT. ☐ DTIC USERS	21. ABSTRACT SECURITY CLASSIFICATION
22a NAME OF RESPONSIBLE INDIVIDUAL Dr. K. J. Wynne	22b. TELEPHONE (Include Area Code) 202-696-4409 22c. OFFICE SYMBOL

DD FORM 1473, 84 MAR 83 APR edition may be used until exhausted. All other editions are obsolete.

SECURITY CLASSIFICATION OF THIS PAGE

DL/413/83/01
GEN/413-2

TECHNICAL REPORT DISTRIBUTION LIST, GEN

	No. Copies
Office of Naval Research Attn: Code 413 800 N. Quincy Street Arlington, Virginia 22217	2
Dr. Bernard Douda Naval Weapons Support Center Code 5042 Crane, Indiana 47522	1
Commander, Naval Air Systems Command Attn: Code 310C (H. Rosenwasser) Washington, D.C. 20360	1
Naval Civil Engineering Laboratory Attn: Dr. R. W. Drisko Port Hueneme, California 93401	1
Defense Technical Information Center Building 5, Cameron Station Alexandria, Virginia 22314	12
DTNSRDC Attn: Dr. G. Bosmajian Applied Chemistry Division Annapolis, Maryland 21401	1
Dr. William Tolles Superintendent Chemistry Division, Code 6100 Naval Research Laboratory Washington, D.C. 20375	1

	No. Copies
Dr. David Young Code 334 NORDA NSTL, Mississippi 39529	
Naval Weapons Center Attn: Dr. Ron Atkins Chemistry Division China Lake, California 93555	
Scientific Advisor Commandant of the Marine Corps Code RD-1 Washington, D.C. 20380	
U.S. Army Research Office Attn: CRO-AA-IP P.O. Box 12211 Research Triangle Park, NC 27709	
Mr. John Boyle Materials Branch Naval Ship Engineering Center Philadelphia, Pennsylvania 19112	
Naval Ocean Systems Center Attn: Dr. S. Yamamoto Marine Sciences Division San Diego, California 91232	1

A-1

A STUDY OF THE ISOTHERMAL CRYSTALLIZATION KINETICS OF POLY[BIS(TRIFLUOROETHOXY)PHOSPHAZENE] AND POLY[BIS(PHENYLPHENOXY)PHOSPHAZENE]

R. J. Ciora Jr. and J. H. Magill

School of Engineering, University of Pittsburgh

Pittsburgh, PA 15261 USA

INTRODUCTION

The most recently developed inorganic based polymers that show considerable commercial potential are the polyphosphazene polymers. In general the polyphosphazene polymers consist of a chain backbone of alternating phosphorous and nitrogen as illustrated in figure 1.

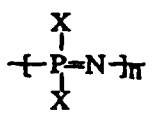

For PBFP $X = OCH_2CF_3$

For PB(4-Ph)PP $X = OPhPh$

Figure 1: The basic alternating phosphorous-nitrogen structure of the poly(phosphazene) polymer.

Common substituents on the phosphorous atom may include aryl, alkyl, aryloxy, alkoxy, amino, halogens as well as several metal atoms and inorganic groups. Different kinds of substituents on the phosphorous atom provide polymers which possess a wide variety of properties[1,2].

Characterization[3,4,5,6,7] of these polymers lags far behind synthesis. Many polyphosphazenes exhibit thermotropic mesophase behavior. However little is known about the mechanisms of crystallization between the various phases under isothermal conditions. Through bulk isothermal crystallization studies, insight into energetics of formation of the various crystalline phases may be ascertained. Recently work has focused on the thermotropic mesophases of small molecules[8,9,10,11,12,13,14,15] and some macromolecules.[16,17,18] The objectives of this research were essentially threefold:

1. to establish and quantify the rate at which these polymers crystallize,
2. to establish the type and/or mode of crystallization by which these polymers crystallize, and
3. to examine the nature and energetics of the crystallization process in these polymers.

EXPERIMENTAL

Materials: In this study two polyphosphazene polymers, poly[bis(trifluoroethoxy)phosphazene], PBFP, and poly[bis(phenylphenoxy)phosphazene], PB(4-Ph)PP, were investigated. Both samples were synthesized via the solution polymerization technique[19]. These two materials were characterized by DSC, X-ray, and ^{31}P solution NMR. The NMR results revealed that neither polymer exhibited crosslinking or branching. Characterization data relevant to PBFP[6] and PB(4-Ph)PP[20] are listed in Table 1.

Equipment: Differential Scanning Calorimetry, DSC, measurements were performed using a calibrated Perkin Elmer DSC-2 equipped with a scanning autozero and interfaced with an IBM-PC for data acquisition. All measurements were performed in a nitrogen atmosphere and a low temperature dry ice/ethanol bath was utilized for rapid thermal equilibration during sample quenching operations. Maximum range sensitivity of 0.1 mcal/sec was used for all experimental determinations. Samples weighed between 8 and 12 mgs. and were sealed in aluminum pans. Isothermal crystallization measurements at several temperatures were carried out by DSC in both the sub T_m and sub T(1) regions for PBFP. No DSC measurements were made for PB(4-Ph)PP.

Light depolarization measurements were carried out using a Hacker Instruments polarizing microscope fitted with a photodiode for measuring light intensity. The signal from the photodiode was amplified via a Phillips PM5170 amplifier and then recorded on a Hitachi Ltd. strip chart recorder. Temperature control of the stage was accomplished using a calibrated Mettler FP-2 hotstage. Nitrogen was used to purge the stage at all times to prevent sample degradation. Samples weighed less than 1 mg. and were placed between glass coverslips. Isothermal crystallization measurements at several temperatures were carried out in both the sub T_m and sub T(1) regions for PB(4-Ph)PP and the sub T_m region for PBFP. In all experiments the sample was fused above its melting temperature, then quenched to the desired crystallization temperature (40°C/min via DSC and ~25°C/min via DLI).

Photomicrographs were taken in the sub T_m region for both PBFP and PB(4-Ph)PP and the sub T(1) region for PB(4-Ph)PP during phase transformations with a Leica 35mm camera using Kodak Tri-X pan (ASA) 400 speed film.

THEORY

To characterize the rate and mode of crystallization, the familiar Avrami equation

$$X(t) = 1-\exp(-kt^n) \tag{1}$$

was used where k is a temperature dependent rate constant, n describes the mode of nucleation and crystal growth and is usually an integer between 1 and 4, and X(t) represents the fraction of transformed or crystallized material after time, t.

In the DSC technique X(t) is expressed as

$$X(t) = \frac{\Delta H_t}{\Delta H_\infty} = \frac{\int_0^t E_t\,dt}{\int_0^\infty E_t\,dt} \tag{2}$$

where ΔH_t is the enthalpy change at time, t, ΔH_∞ is the total enthalpy change of the system, and

E_t is the rate of energy evolution at time, t.

In the depolarized light intensity[21] (DLI) technique it is expressed as

$$X(t) = \frac{I_\infty - I_t}{I_\infty - I_o} \tag{3}$$

where I_∞, I_o, and I_t represent the transmitted light intensity at long time, initial time, and at time, t. Avrami theory is useful for determining the macroscopic mode of crystal nucleation (heterogeneous or homogeneous), the crystal growth habit (spherical, circular, etc.), and the overall rate at which crystallization proceeds.

Crystallization in polymeric materials is generally nucleation controlled. By means of classical nucleation theory the energetics of formation of the nuclei are examined. Turnbull and Fisher[22] have shown the rate at which nucleation occurs at constant temperature and pressure is given by:

$$N = N_o \exp(-\Delta E/k_b T_c)\exp(-\Delta G^*/k_b T_c) \tag{4}$$

where N is the nucleation rate, N_o is a pre-exponential temperature independent constant, ΔE is the temperature dependent energy of activation for transport from the isotropic phase, ΔG^* is the critical free energy of the critical sized nuclei, and k_b and T_c are the Boltzmann constant and the crystallization temperature, respectively. In general ΔE is roughly constant at small undercooling compared to the temperature dependence of ΔG^*. The equation is basic to primary and/or secondary nucleation.

If the linear crystal growth rate, G, is assumed a nucleation controlled process, then nucleation theory may be utilized to describe the linear growth rate of the crystalline phase as

$$G = G_o \exp(-\Delta E/k_b T_c)\exp(-\Delta G^*_g/k_b T_c) \tag{5}$$

where ΔG^*_g is the free energy of formation of the secondary nuclei. ΔG^* or ΔG_g^* has been evaluated by several authors. Table 2 shows various functions for ΔG^* for different modes of nucleation specifically, 3-D and 2-D heterogeneous and homogeneous primary nucleation based on a rectangular equilibrium shape. Also shown is the equation for secondary nucleation via the coherent, heterogeneous mechanism.

In the absence of independent values of N and G, the Avrami temperature dependent rate parameter, k, may be utilized, through the relationship

$$k \sim NG^z \tag{6}$$

where z is the growth dimensionality of the macroscopic crystallites. From equations 4 and 5 it is possible to generate an equation of the form,

$$\ln k \sim C_o - \Delta G^*/k_b T_c - \frac{4zb_o\sigma\sigma_e T_m^o}{k_b \Delta H T_c \Delta T} \tag{7}$$

where C_o is a constant embodying the transport terms as well as G_o and N_o. Information about the surface free energies of the critical nuclei may be obtained from the slope of a plot of ln k versus $1/T_c\Delta T$ or $1/T_c\Delta T^2$.

The limitations of both the Avrami and classical nucleation theories with respect to polymeric systems have been documented[23], but, within the scope of these restrictions, it is possible to gain

insights into the mechanics and energetics of the crystallization transformations in such systems.

RESULTS AND DISCUSSION

Transformations in PBFP

(a) Isotropic Melt to 2-D Region: The Avrami plots of this transformation obtained via the DSC method are shown in figure 2. Significant curvature is introduced in these plots at short times and low conversions if the rate of energy evolution, E_t, is not measured properly. This problem is a result of fluctuations in the energy signal from the DSC at short times (~ 30 to 120 seconds) following mode switching operations, specifically from cooling to isothermal or isothermal to heating operations. An isothermal baseline subtraction technique and an extent of conversion recovery technique (based on comparing heats of fusion corresponding to crystallizations done at short times compared to those done at long times), were employed to correctly predict the short time extent of conversion. This significantly reduced the initial curvature that would result in the low conversion end of the Avrami plots. From linear least square fits of the data in the initial linear portion of each curve, an average value of n was determined to be 2.06 ± 0.11. Approximating a value of n of 2.0, values of k, expressed as $sec^{-2.0}$, were calculated at a fractional conversion of 0.25. Avrami plots from the DLI measurements for the transformation are shown in figure 3. The average value of n was determined to be 1.93 ± 0.07 (by least square). Again the rate parameters, k, were evaluated at a fractional conversion of 0.25 with n approximated as 2.

Photomicrographs of this transformation showed the primary nucleation to be heterogeneous. Considering both the DSC and DLI techniques provided an n ~ 2 for this transformation, it may be concluded that the growth habit of the crystallites is two dimensional from heterogeneous nuclei.

Plots of ln k versus $1/T_c\Delta T$ and $1/T_c\Delta T^2$ are illustrated in figures 4 and 5 for the DSC and DLI methods, respectively. At comparable crystallization temperatures, k values obtained by the DSC and DLI methods are in agreement. The temperature dependence of k is both extremely large and negative, decreasing four orders of magnitude in a crystallization range of 6°C. This large temperature dependence of k suggests nucleation control for the overall transformation to the 2-D phase.

Only from the DLI data is it readily apparent that the plot versus $1/T_c\Delta T$ is linear. The slopes of the plots of ln k versus $1/T_c\Delta T$ obtained via the DSC and DLI techniques were -74,900 and -96,100 K^2, respectively. Assuming that 2-D heterogeneous primary nucleation is applicable for the calculation of the surface energies of the critical nuclei, then $\Delta G^* = 4l^2\Delta\sigma\sigma/(l\delta f - 2\sigma_e)$ may be applied to equation 7, yielding an equation of the form,

$$\ln k \sim C_o - \left\{\frac{4l^2\Delta\sigma\sigma T^o{}_m}{l\Delta H\Delta T - 2\sigma_e} + \frac{4zb_o\sigma\sigma_e T^o{}_m}{\Delta H\Delta T}\right\}\left\{\frac{1}{k_b T_c}\right\} \tag{8}$$

Two conditions apply to explain the linearity of the plots of ln k versus $1/T_c\Delta T$, specifically (i) when $2\sigma_e << l\delta f$ or (ii) when $\sigma\Delta\sigma << \sigma\sigma_e$. The first condition is inappropriate, since it can be shown that for $2\sigma_e \sim 0.1 l\delta f$, σ would be less than $\Delta\sigma$ and homogeneous primary nucleation would be favored over heterogeneous nucleation. This is not borne out in the photomicrographs nor in most crystallization studies of normal homopolymers at such small undercoolings. The second condition results when primary nucleation occurs in cracks, folds, ledges, etc., as opposed to a

flat substrate. This would reduce the surface energy product, $\sigma\Delta\sigma$, in the second term, so ln k would be dominated by the third term (the linear growth term). Photomicrographs of the transformation show the number of nuclei does not increase substantially compared to the growth rate as temperature is lowered over the crystallization temperature range investigated. Thus the linear growth rate appears more sensitive to temperature than the primary nucleation density over this narrow temperature range, suggesting that $\sigma\sigma_e >> \sigma\Delta\sigma$, and equation 8 then reduces to:

$$\text{slope} = -8b_o\sigma\sigma_e T^o_m/k_b\Delta H \qquad (9)$$

Here, for PBFP, $\Delta H = 1.53$ cal/cm^3, $b_o = 11.8$ Å, and $z = 2$, since the results from the Avrami analysis indicate the growth is two dimensional. If the average value of the slope is determined (-85500 K^2), the product of the surface free energies, $\sigma\sigma_e$, is 1.55 ergs^2/cm^4. The product of the surface energies[24] from linear growth rate experiments for many common homopolymers are at least two orders of magnitude greater than the value determined here for PBFP.

(b) 2-D to 3-D Region: Figure 6 shows Avrami plots of this data. By least squares fit of the data in the initial linear portion of each curve an average value of $n=1.91\pm0.08$ was obtained. Values of k were determined utilizing an estimated value of $n = 2.0$ and a fractional transformation of 0.2. Unlike the isotropic melt to 2-D transformation in PBFP, this transformation displayed a small birefringence change and therefore was not readily amenable to measurement by the DLI method. It was also impossible to calculate a nucleation density or the linear growth rate from photomicrographs in this region. Plots of ln k versus $1/T_c\Delta T$ and $1/T_c\Delta T^2$, were made for this transition and are shown in figure 7. The low supercooling portion of the plot versus $1/T_c\Delta T$ yielded a slope of -67,400 K^2. This large, negative change in the rate constants over this small crystallization range in addition to the small undercooling needed for crystallization indicates the nucleation was heterogeneous. Coupled with an Avrami nucleation parameter of 2, it may be concluded that the growth occurs in two dimensions.

Two important points may be made about this transition. First, at comparable undercoolings from their respective transition temperatures, the 2-D to 3-D transformation takes place at a rate that is an order of magnitude faster than in the isotropic to 2-D transformation. Second, over the measurable crystallization range (1.2°C), the rate constant k changes by two orders of magnitude. For extrapolation to a temperature range of 6°C (DLI measurement range for the isotropic to 2-D transformation), a change in k of over 5 orders of magnitude is expected. It is this fact that leads to the conclusion that the crystallization transformation is nucleation controlled. From the slope of the high temperature end of the plot of ln k versus $1/T_c\Delta T$, the value of the product of the surface free energies, $\sigma\sigma_e$ was determined to be 30.1 ergs^2/cm^4 for $\Delta H = 21.1$ cal/cm^3, $b_o = 9.4$ Å, and again $z = 2$. Although this value is larger than the value obtained for the isotropic to mesophase transformation, it is still at least an order of magnitude less than that obtained for normal homopolymers of comparable enthalpy of transformation.

Transformations in PB(4-Ph)PP

(a) Isotropic Melt to 2-D Transformation: Avrami plots of the data for this transformation are shown in Figure 8. An average value of $n = 2.02\pm0.12$ was obtained for the nucleation parameter. Photomicrographs of this transformation showed the primary nucleation to heterogeneous. These factors indicate that the growth geometry of the crystallites is two dimensional in nature. Values for k were determined at a fractional conversion of 0.3 for an n of

2. Plots of ln k versus $1/T_c\Delta T$ and $1/T_c\Delta T^2$ are shown in figure 9. As is apparent the rate constants increase substantially over the small crystallization range as the undercooling increases, and this behavior is attributable to nucleation control of the transformation via the primary and/or secondary nucleation steps. Since the plot of ln k vs. $1/T_c\Delta T$ is linear, yielding a slope of -253,000, equation 9 was used to analyze the data. The product of the surface free energies, $\sigma\sigma_e$, is 5.0 $ergs^2/cm^4$, for ΔH = 1.95 cal/cm^3 and b_o = 18.1 Å. Here $\sigma\sigma_e$ is of the same order of magnitude as in PBFP and is several orders of magnitude below that found for normal homopolymers.

Although PBFP and PB(4-Ph)PP display similar mechanisms for the isotropic to 2-D transformation, a significantly larger undercooling is necessary to drive the transformation in PB(4-Ph)PP. This is also reflected in the product of the surface free energy terms which indicate that less energy is needed to overcome the barriers to nucleation in PBFP compared to PB(4-Ph)PP. Obviously the -phenylphenoxy side group, being much bulkier than the -trifluoroethoxy sidegroup, inhibits the incorporation of new chains into a crystalline lattice.

(b) 2-D to 3-D Transformation: Avrami n and k data for this transformation were generated from the Avrami plots of figure 10. An average n of 2.08±0.12 was obtained and values of k were determine at a fractional conversion of 0.25. Plots of ln k vs $1/T_c\Delta T$ and $1/T_c\Delta T^2$ were made and are shown in figure 11. The low supercooling end of the plot versus $1/T_c\Delta T$ yielded a slope of -189,000 K^2. As shown the rate constants for this transformation increase significantly with increasing undercooling. This behavior is characteristic of nucleation controlled crystal growth and is associated with heterogeneous nucleation. This factor coupled with an n of 2 indicates the growth occurs two dimensionally from heterogeneous nuclei as found in PBFP.

Utilizing equation 9 the surface free energy product, $\sigma\sigma_e$, was estimated to be 42.1 $ergs^2/cm^4$ for ΔH = 27.7 cal/cm^3, b_o = 18.3 Å, and z = 2. This product is, as for the same transformation in PBFP, larger than that obtained for the isotropic to 2-D mesophase transition, yet is at least an order of magnitude less than that obtained for the isotropic to crystalline transformation in normal homopolymers of comparable enthalpy of transition.

Compared to PBFP, PB(4-Ph)PP crystallizes at larger undercoolings with a smaller change in rate over a comparable crystallization temperature range, and the surface free energy product for PB(4-Ph)PP is larger than that obtained for PBFP for this transition. Consequently, the -phenylphenoxy side group, which is bulkier than the -trifluoroethoxy side group, inhibits crystallization, a result similar to the isotropic to 2-D transformation.

CONCLUSIONS

The mechanisms for the nucleation and growth of PBFP and PB(4-Ph)PP have been established for (1) the isotropic to 2-D thermotropic mesophase and for (2) the 2-D thermotropic mesophase to 3-D crystal transformations. The product of the surface free energies, $\sigma\sigma_e$, for both transformations have been estimated to be at least an order of magnitude less than the values usually observed for the isotropic to crystalline transformation in normal homopolymers. The small undercoolings necessary to crystallize these samples and the extremely large dependence of the rate parameter on undercooling indicate that relatively small forces must be overcome for the crystallization of these polymers in both transformation regions.

Difficulties encountered in measuring crystallization transformations using the DSC technique have been mitigated by procedures introduced in this work, namely the short time extent of conversion recovery using a (i) baseline subtraction technique and (ii) a recrystallization/reheating technique. This article shows that the initial portion of crystallization may be recovered satisfactorily. In general the techniques should have wide application for kinetic measurements using the DSC.

ACKNOWLEDGMENTS

Thanks are due to the National Science Foundation (Polymer Program. Grant # DMR 8509412) and the Office of Naval Research (Chemistry Program, Grant # N0001485K0358) for research support. The authors also wish to thank Dr. T. Nishikawa of the Nippon Soda Company for supplying the polymerization grade trimer used for the synthesis of these polyphosphazenes.

References

1. Singler, R. E. and Hagnauer, G. L., *Polyphosphazenes: Structure and Applications*, Academic Press, New York, 1978.
2. Allcock, H. R., Fuller, T. J., Matsumura K., and Austin, P. E., "", *Polymer Preprints*,Vol. 21 1983, pp. 111-112.
3. Peddada, S. V. and J. H. Magill, *Macromolecules*,Vol. 16 1983, pp. 1258-1264.
4. Sun, D. C. and Magill, J. H., *Polymer Papers*,Vol. 28 1987, pp. 1243-1252.
5. Choy, I. C. and Magill, J. H., *J. Poly. Sci.: Chem.*,Vol. 19 1981, pp. 2495-2518.
6. Kojima, M. and Magill, J. H., *Polymer*,Vol. 26 1985, pp. 1971-1978.
7. Alexander, M. N., and Desper, C. R., Sagalyn, P. L., and Schneider, N. S., *Macromolecules*,Vol. 10 1977, pp. 721-724.
8. Price, F. P. and Wendorf J. H., *J. Phys. Chem.*,Vol. 75 1971, pp. 2839-2849.
9. Price, F. P. and Wendorf J. H., *J. Phys. Chem.*,Vol. 75 1971, pp. 2849-2853.
10. Price, F. P. and Wendorf J. H., *J. Phys. Chem.*,Vol. 76 1972, pp. 276-280.
11. Price, F. P. and Fritzsche, K., *J. Phys. Chem.*,Vol. 77 1973, pp. 386-399.
12. Jabarin, S. A. and Stein, R. S., *J. Phys. Chem.*,Vol. 77 1973, pp. 399-408.
13. Jabarin, S. A. and Stein, R. S., *J. Phys. Chem.*,Vol. 77 1973, pp. 409-413.
14. Adamski, P. and Czyzewski, R., *Sov. Phys. Crystallogr.*,Vol. 23 1978, pp. 82-85.
15. Adamski, P. and Czyzewski, R., *Sov. Phys. Crystallogr.*,Vol. 22 1978, pp. 725-726.
16. Warner, S. B. and Jaffe, M., *J. of Crystal Growth*,Vol. 48 1980, pp. 184-190.
17. Grebowicz, J., Cheng, S. Z. D., and Wunderlich, B., *J. of Poly. Sci.: Part B: Poly. Phys.*,Vol. 24 1986, pp. 675-685.
18. Liu, X., Hu, S., Xu, M., Zhou, Q., and Duan, X., *Polymer*,Vol. 30 1989, pp. 273-279.
19. Mujumdar, A., Master's thesis, University of Pittsburgh, 1988.
20. Kojima, M., "private communication".
21. Magill, J. H., *Nature*,Vol. 187 1960, pp. 770-771.

22. Turnbull, D. and Fisher, J. C., *J. Chem. Phys.*,Vol. 17 1949, pp. 71-74.

23. Wunderlich B., *Macromolecular Physics Vol. 2*, Academic Press, New York, 1976.

24. Hoffman, J. D., Davis, G. T., and Lauritzen, J. I. Jr., *Treatise on Solid State Chemistry*, Plenum Press, New York, 1972.

Table 1: Characterization data of the two samples, PBFP and PB(4-Ph)PP.

		PBFP	DPP
density (γ - form)*		1.7 g/cm³	1.3 g/cm³
unit cell dimensions (γ-form)	a_o	20.60 Å	41.8 Å
	b_o	9.40 Å	18.3 Å
	c_o	4.86 Å	9.57 Å
unit cell dimensions (hexagonal form)**	$a_{(200)}$	11.8 Å	18.1 Å
mesophase transition temperature, T(1)		89.5 °C	218.2 °C
melting transition temperature, T_m		244.1 °C	280.3 °C
fictive temperature$, T_f		-66.0 °C	52.0 °C
ΔH_f at T_m		0.9 cal/g	1.5 cal/g
ΔH_f at T(1)		12.4 cal/g	21.3 cal/g

* γ - form designates the 3-D orthorhombic structure of many of the poly(phosphazene) polymers.
** hexagonal form designates the general structure of the 2-D mesophase of these polymers.
$ measured after quenching from above the glass transition temperature, then reheating at 10 °C/min.

Table 2: Functions for ΔG^* for several modes of nucleation based on a rectangular equilibrium shape.

3-D Primary Nucleation

$$\Delta G^*_{hom} = 32\sigma^2\sigma_e/\delta f^2$$

$$\Delta G^*_{het} = 32\sigma\Delta\sigma\sigma_e/\delta f^2$$

2-D Primary Nucleation

$$\Delta G^*_{het} = \frac{4l^2\sigma\Delta\sigma}{l\delta f - 2\sigma_e}$$

$$\Delta G^*_{hom} = \frac{4l^2\sigma^2}{l\delta f - 2\sigma_e}$$

Coherent Secondary Nucleation

$$\Delta G^*_g = 4b_o\sigma\sigma_e/\delta f$$

where

$$\delta f = \Delta H_f \Delta T/T_m^o$$

Figure Legends

Figure 1: The basic alternating phosphorous-nitrogen structure of the poly(phosphazene) polymer.

Figure 2: DSC Avrami plots for the isotropic to 2-D mesophase transition of PBFP.

Figure 3: DLI Avrami plots for the isotropic to 2-D mesophase transformation of PBFP.

Figure 4: Plots of ln k versus $1/T_c\Delta T$ and $1/T_c\Delta T^2$ for the isotropic melt to 2-D transformation of PBFP (DSC method).

Figure 5: Plots of ln k versus $1/T_c\Delta T$ and $1/T_c\Delta T^2$ for the isotropic melt to 2-D transformation of PBFP (DLI method).

Figure 6: DSC Avrami plots for the 2-D hexagonal to 3-D orthorhombic transition of PBFP.

Figure 7: Plots of ln k versus $1/T_c\Delta T$ and $1/T_c\Delta T^2$ for the 2-D to 3-D transformation of PBFP.

Figure 8: DLI Avrami plots for the isotropic to mesophase transformation of PB(4-Ph)PP.

Figure 9: Plots of ln k versus $1/T_c\Delta T$ and $1/T_c\Delta T^2$ for the isotropic melt to 2-D transformation of PB(4-Ph)PP.

Figure 10: DLI Avrami plots for the 2-D mesophase to 3-D fully ordered crystal crystallization transformation in PB(4-Ph)PP.

Figure 11: Plots of ln k versus $1/T_c\Delta T$ and $1/T_c\Delta T^2$ for the 2-D to 3-D transformation of PB(4-Ph)PP.

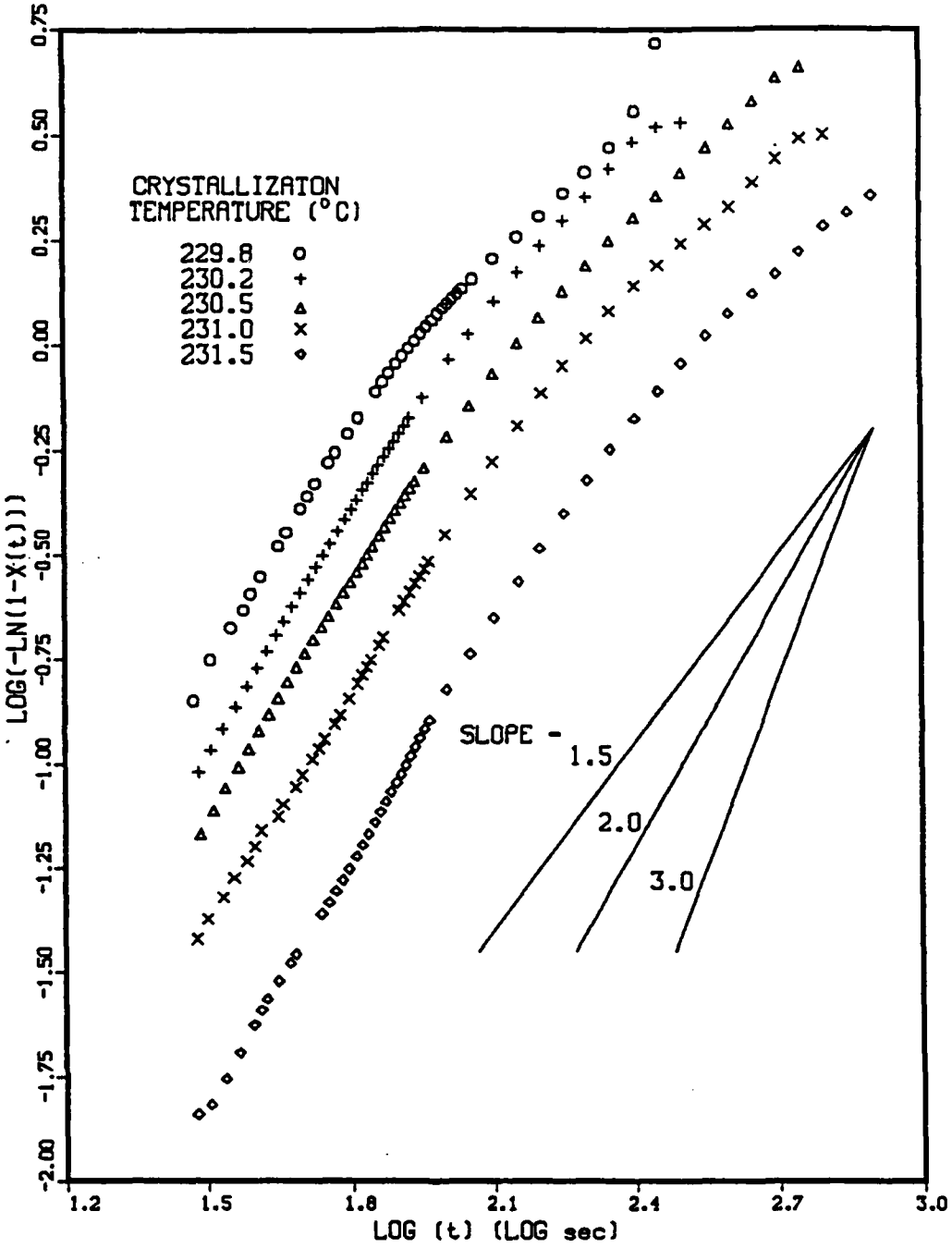

Figure 2: Avrami plots for the given crystallization temperatures for the isotropic to 2D mesophase transition of PBFP via the DSC method.

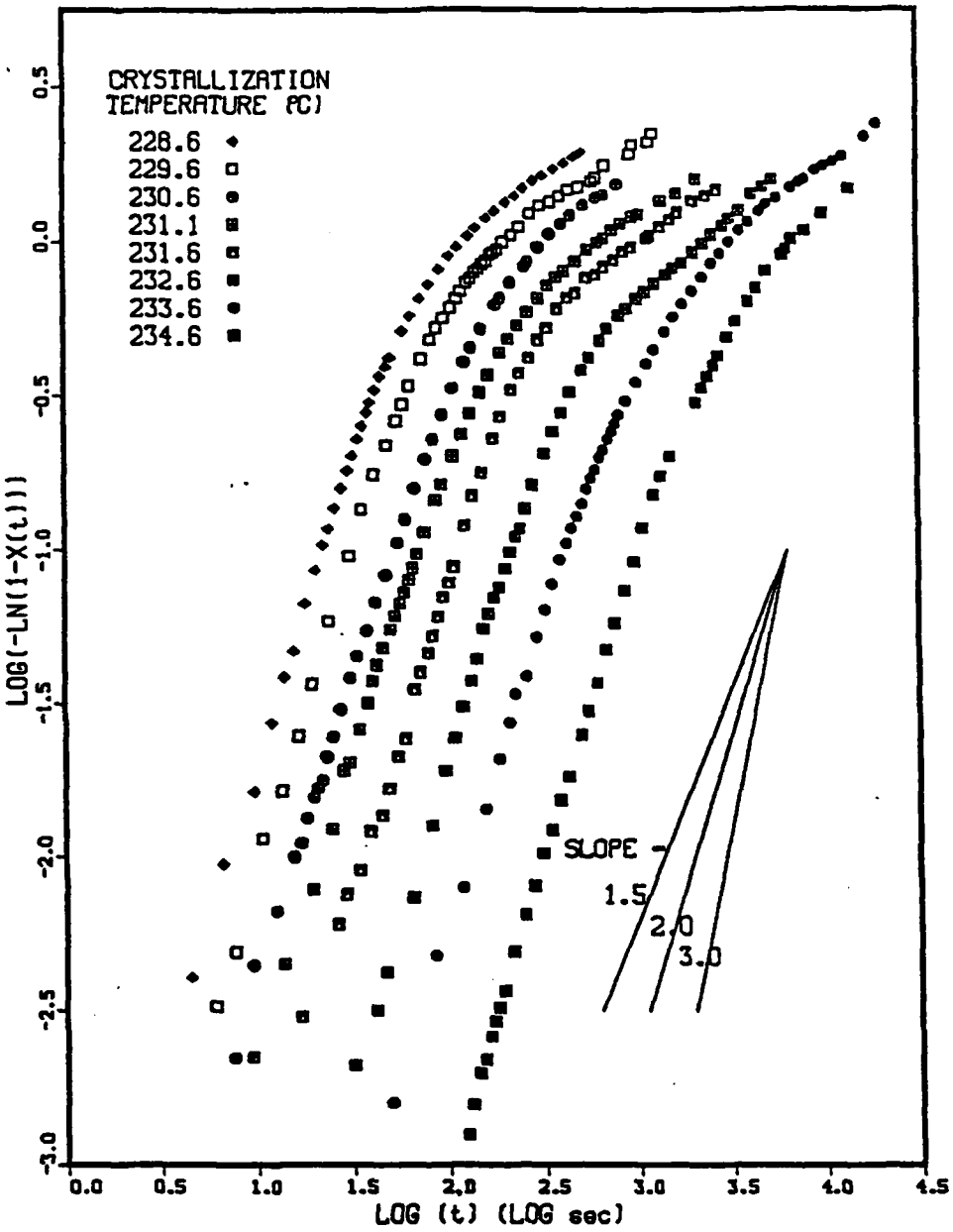

Figure 3: **Avrami plots for the various crystallization temperatures shown for the isotropic to 2-D mesophase transformation of PBFP for the DLI method.**

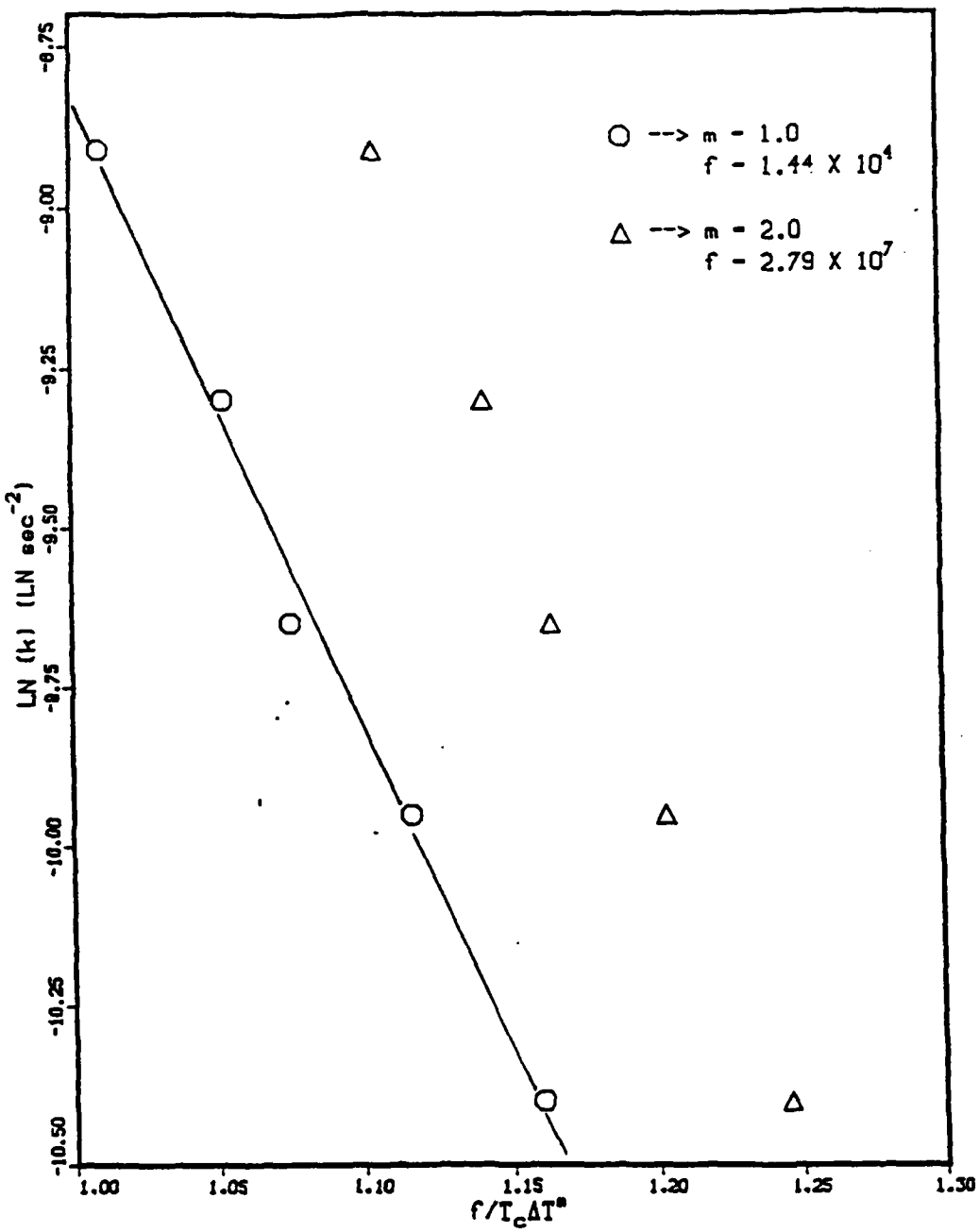

Figure 4: **Plots of ln k versus $1/T_c\Delta T$ and $1/T_c\Delta T^2$ for the isotropic melt to 2-D transformation of PBFP (DSC method). Values**

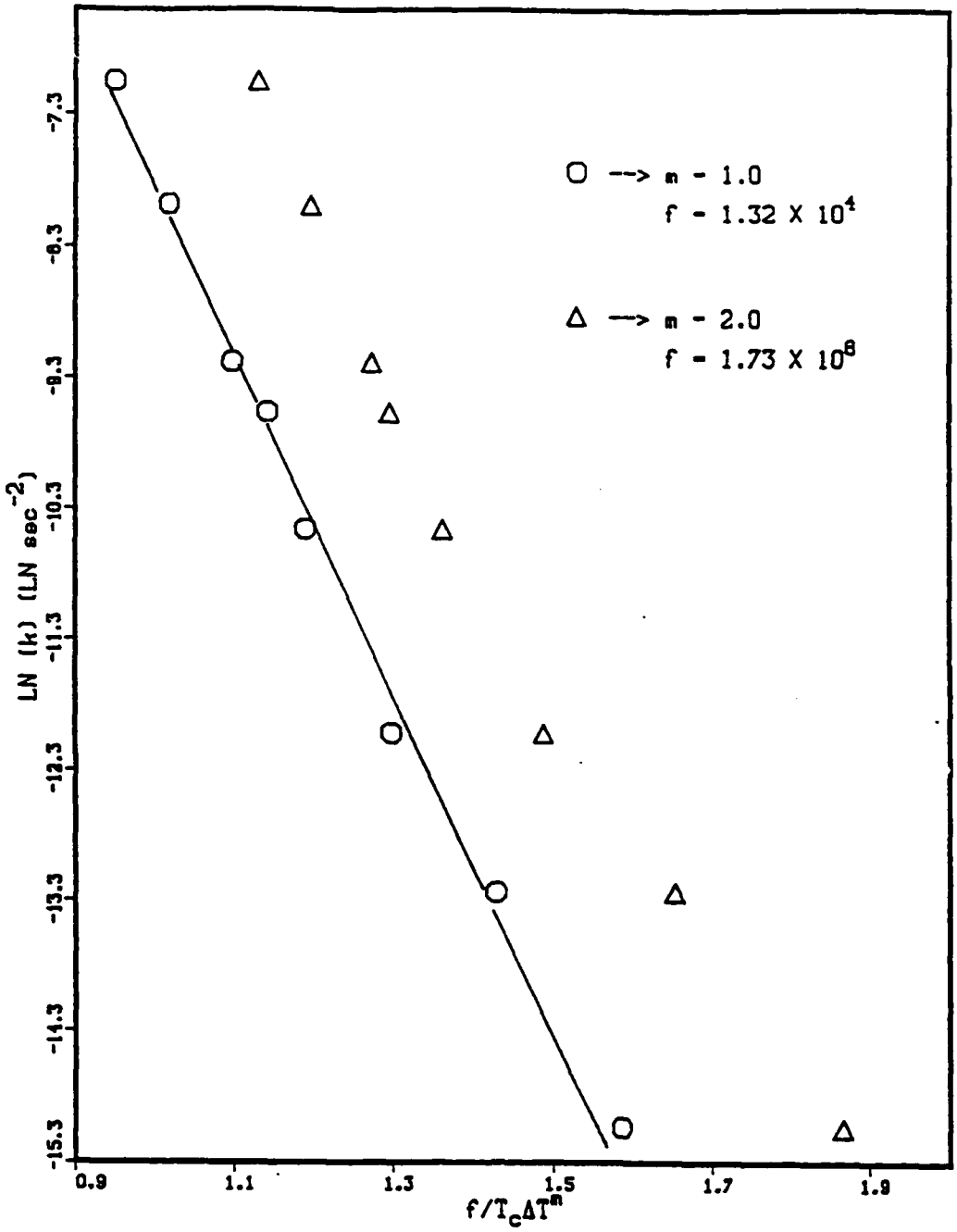

Figure 5: Plots of ln k versus $1/T_c\Delta T$ and $1/T_c\Delta T^2$ for the isotropic melt to 2-D transformation of PBFP (DLI method).

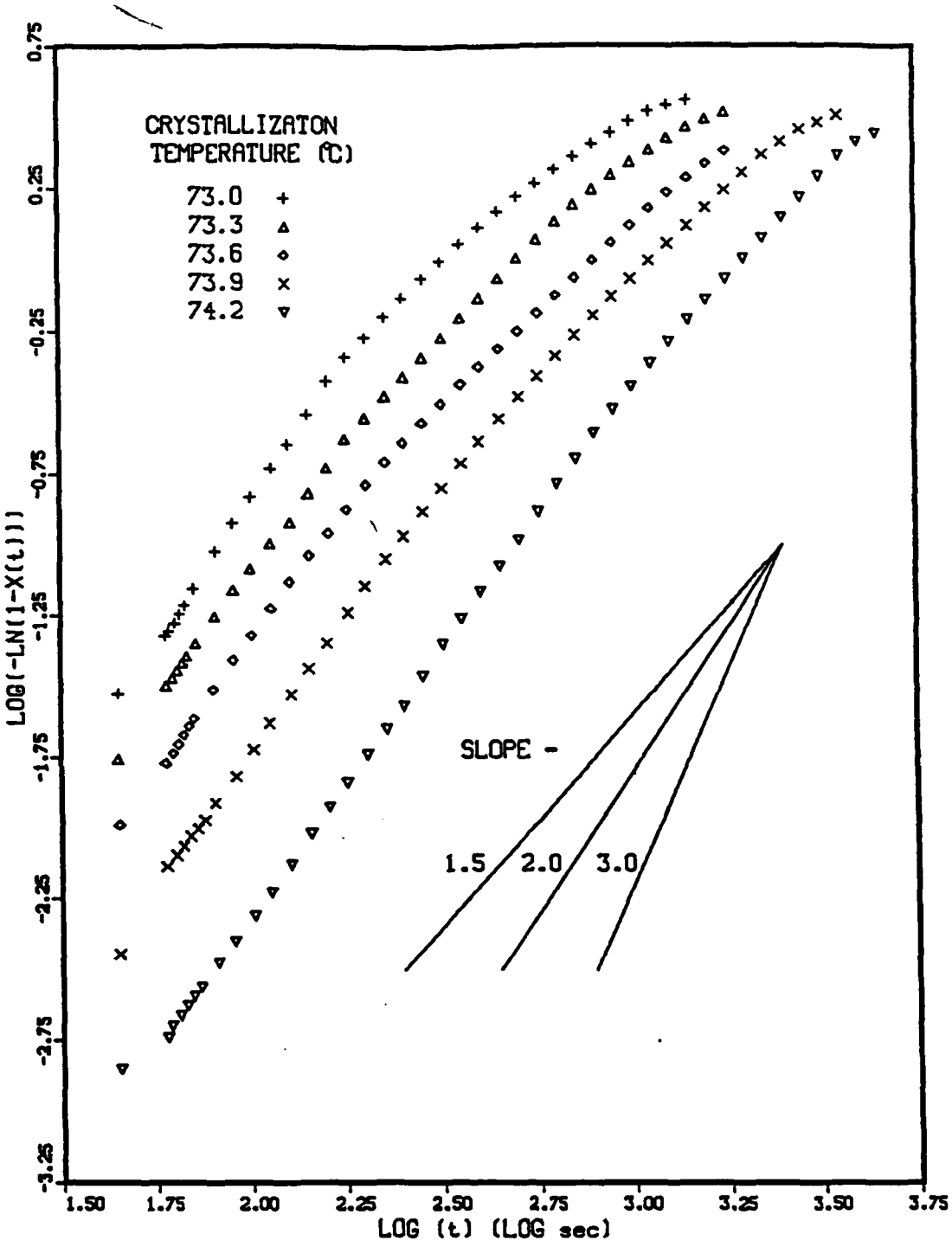

Figure 6: : **Avrami plots for the various crystallization temperatures shown for the 2-D hexagonal to 3-D orthorhombic transition of PBFP.**

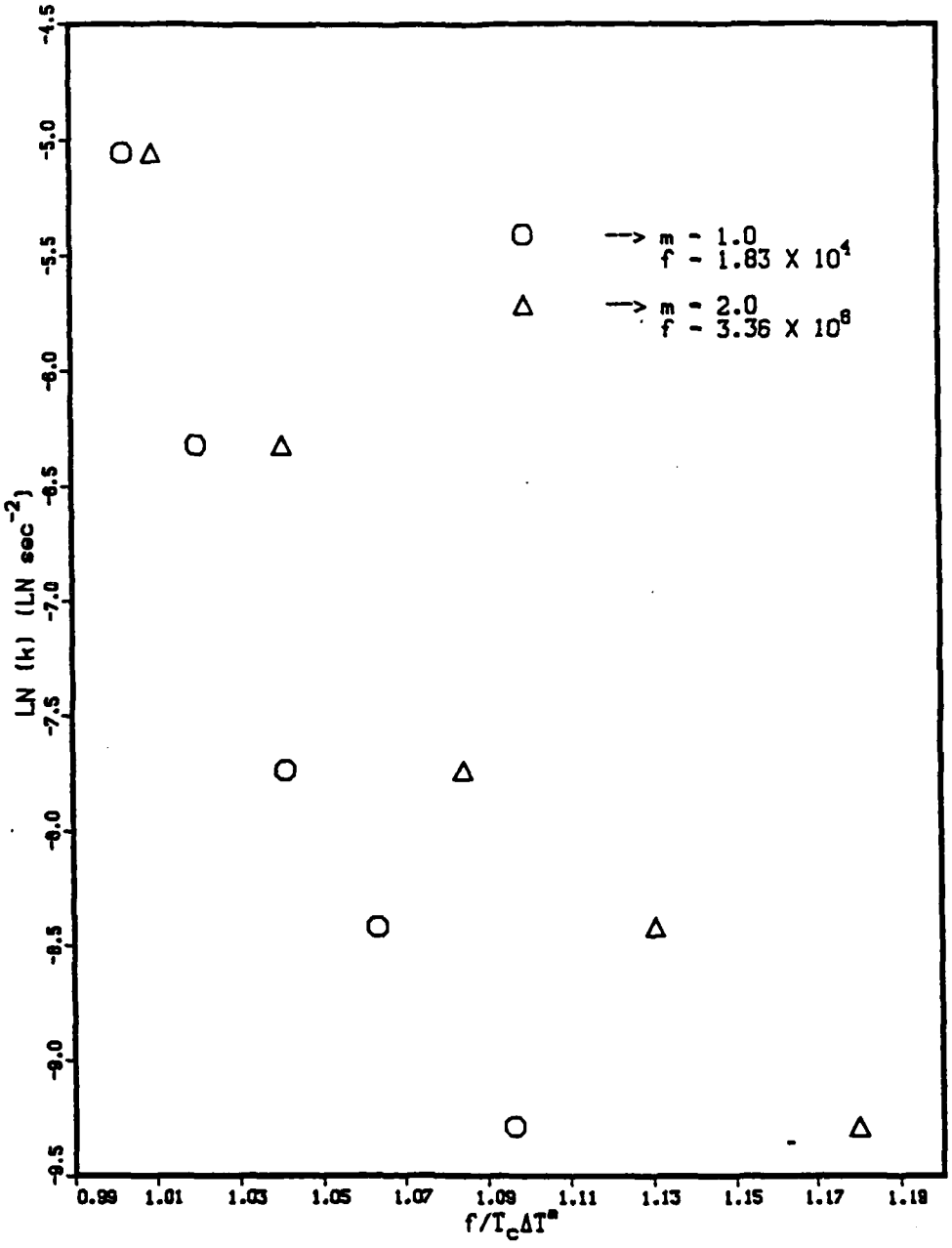

Figure 7: **Plots of ln k versus $1/T_c\Delta T$ and $1/T_c\Delta T^2$ for the 2-D to 3-D transformation of PBFP.**

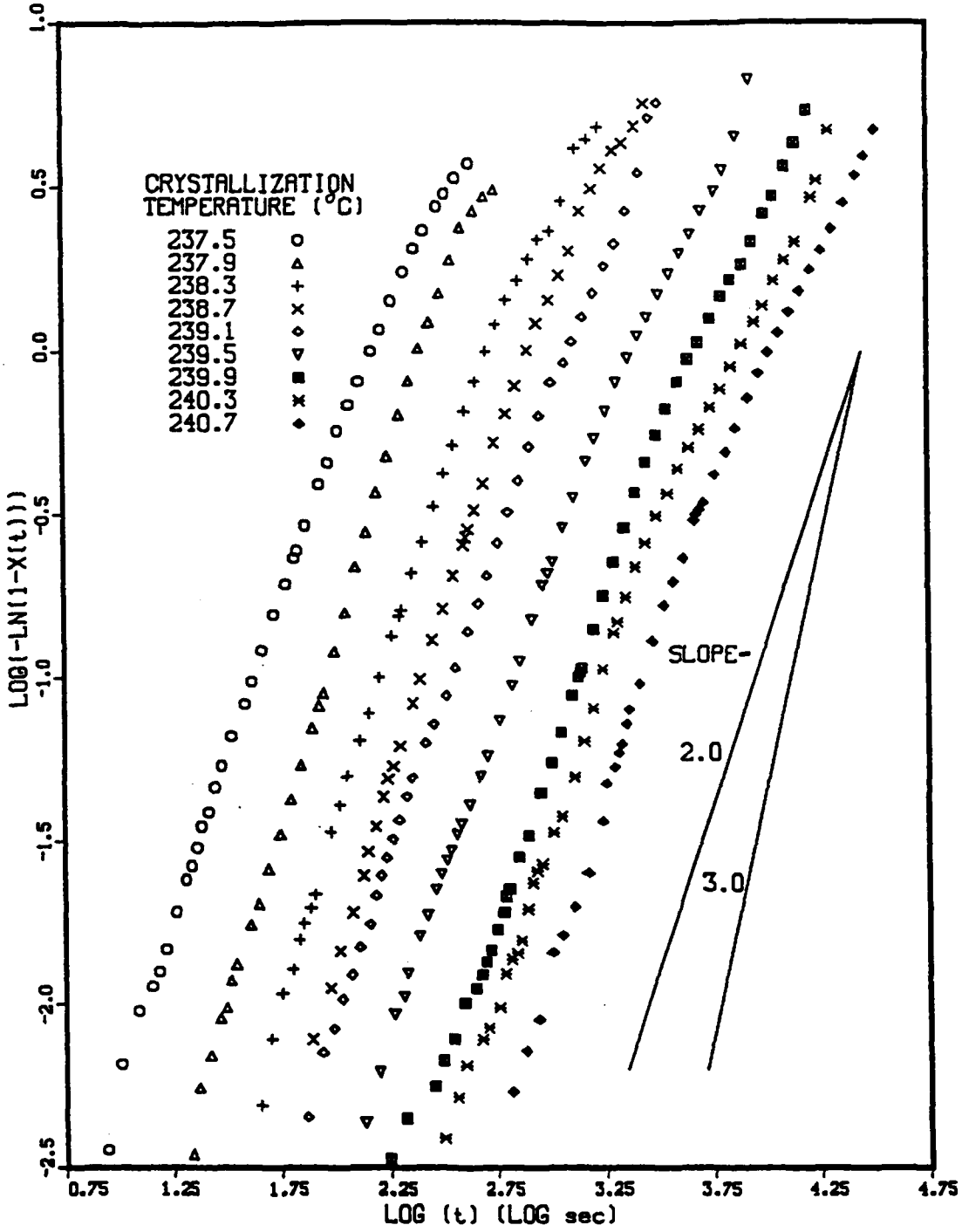

Figure 8: **Avrami plots for the various crystallization temperatures shown for the isotropic to mesophase transformation of DPP via the DLI method.**

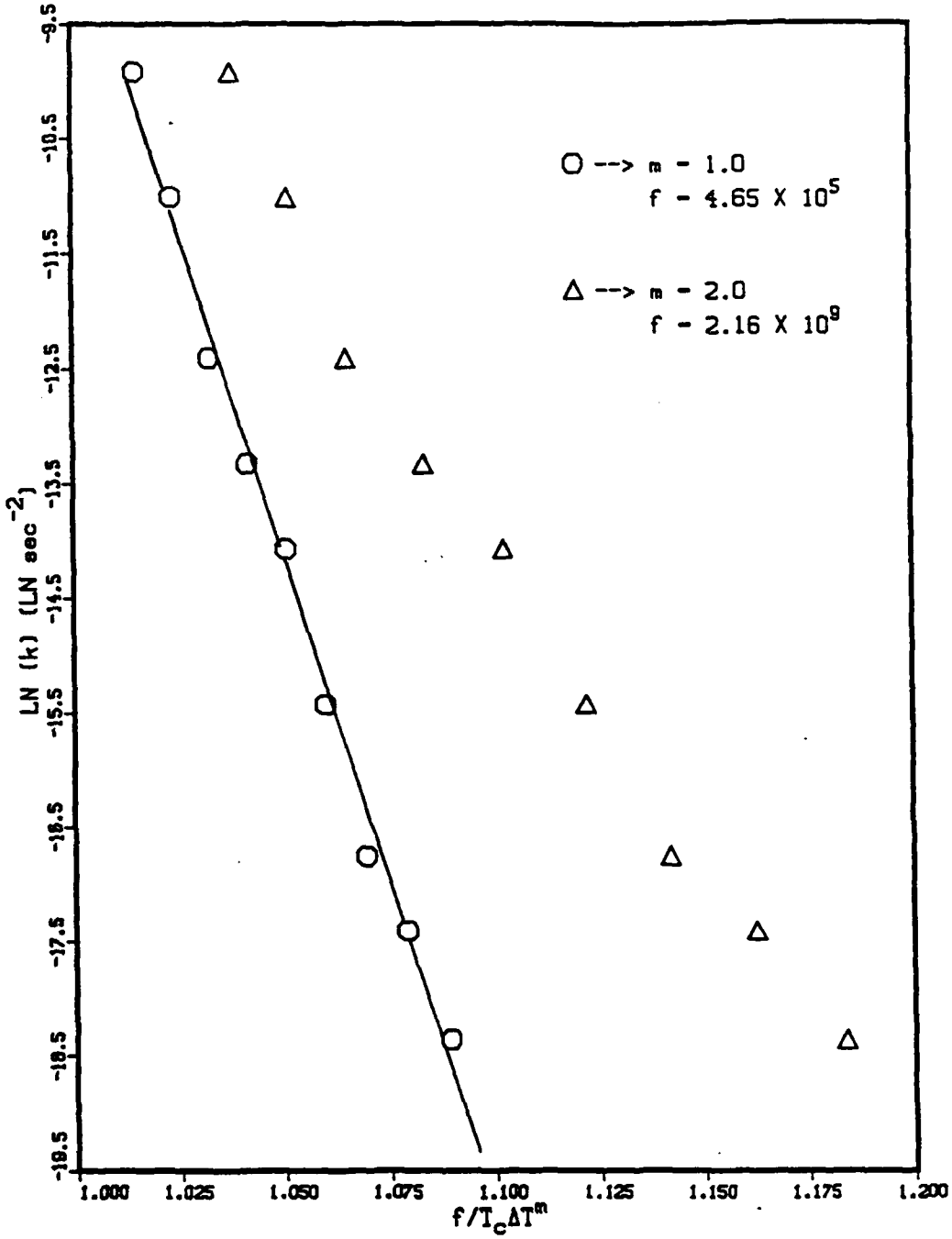

Figure 9: **Plots of ln k versus $1/T_c\Delta T$ and $1/T_c\Delta T^2$ for the isotropic to 2-D mesophase transformation of DPP.**

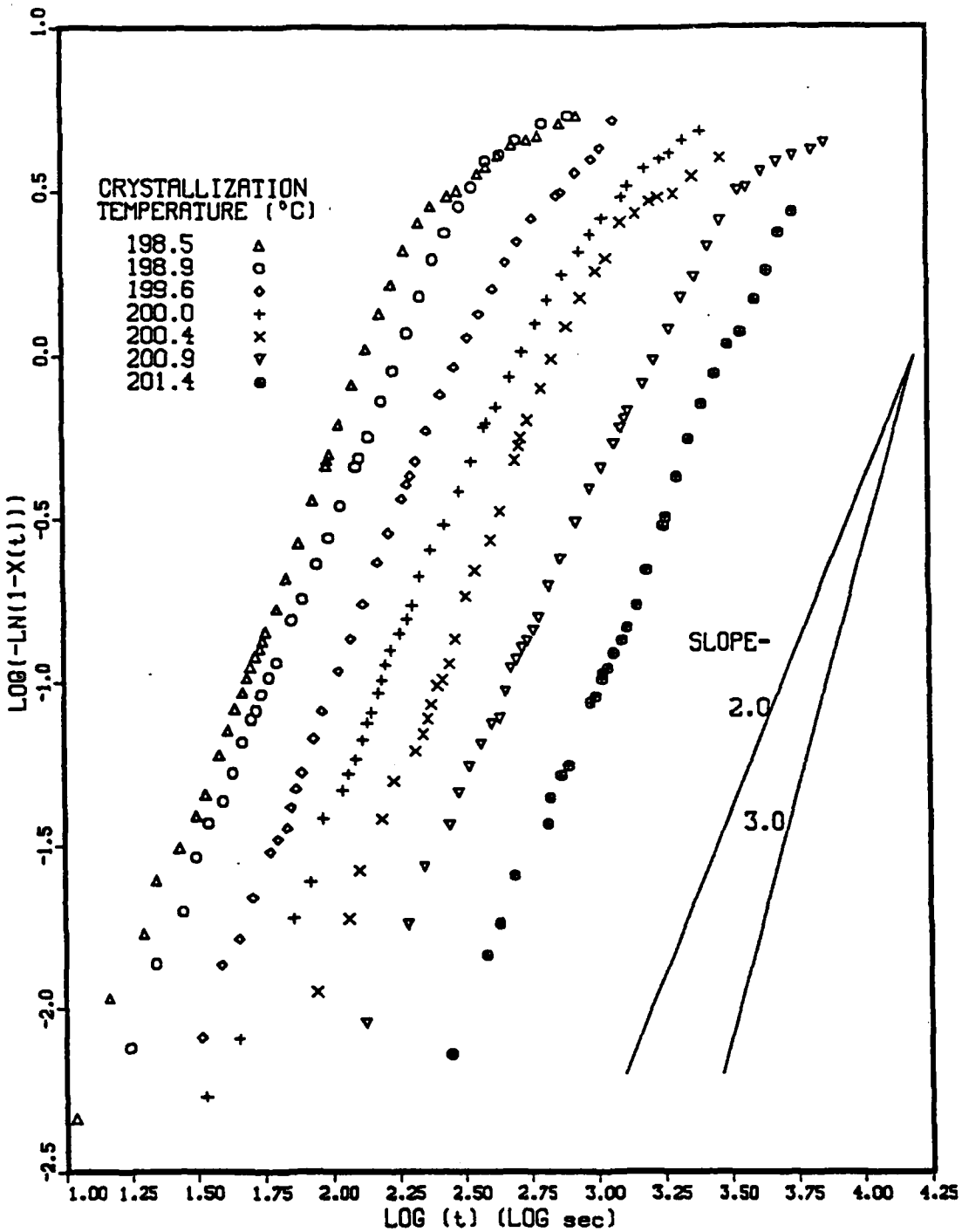

Figure 10: **Avrami plots for the various crystallization temperatures shown for the 2-D mesophase to 3-D fully ordered crystal crystallization transformation of DPP obtained via the DLI method.**

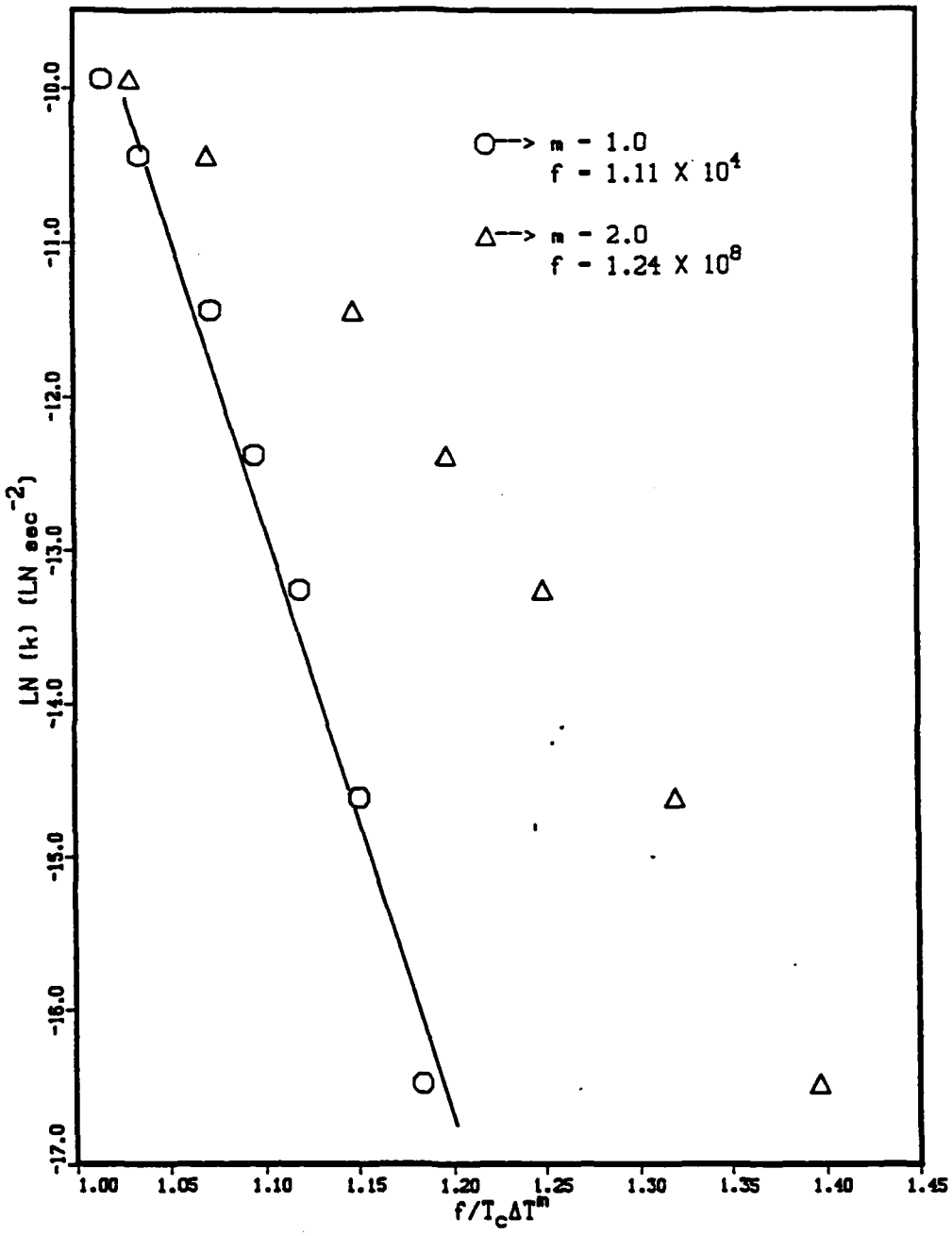

Figure 11: Plots of ln k versus $1/T_c\Delta T$ and $1/T_c\Delta T^2$ for the 2-D to 3-D transformation of DPP.

END
6-89
DTIC